Scalable and Uniform 1D Nanoparticles by Synchronous Polymerisation, Crystallisation, and Self-Assembly

*By Charlotte E. Boott[†], Jessica Gwyther[†], Robert L. Harniman, Dominic W. Hayward and Ian Manners**

[†]These authors contributed equally to this work.

School of Chemistry, University of Bristol, Cantock's Close, Bristol, BS8 1TS, U.K.

*Email: ian.manners@bristol.ac.uk

The preparation of well-defined nanoparticles based on soft matter using solution-processing techniques on a commercially viable scale is a major challenge of widespread importance. Self-assembly of block copolymers in solvents that selectively solvate one of the segments provides a promising route to core-corona nanoparticles (micelles) with a wide range of potential uses. Nevertheless, significant limitations to this approach also exist. For example, the solution processing of block copolymers generally follows a separate synthesis step and is normally performed at high dilution. Moreover, non-spherical micelles, which are promising for many applications, are generally difficult to access, samples are polydisperse, and precise dimensional control is not possible. Herein we demonstrate the formation of platelet and cylindrical micelles at concentrations up to 25% solids via a one-pot approach starting from monomers that combines polymerisation-induced and crystallisation-driven self-assembly. We also show that performing the procedure in the presence of small seed micelles allows the scalable formation of low dispersity samples of cylindrical micelles of controlled length up to 3 microns.

The solution processing of block copolymers (BCPs) with amorphous core-forming segments provides a convenient and important route to core-corona nanoparticles (micelles) with a range of morphologies and functionalities[1,2]. This has resulted in a variety of actual and potential applications as drug delivery vehicles, surfactants, gelators, structure-directing templates, stabilisers, nanowires and also in nanolithography and composite reinforcement[3-7]. Nevertheless, significant drawbacks also exist. For example, the solution processing of BCPs is almost always carried out in a post-polymerisation step that involves addition of a block selective solvent to a unimer (molecularly dissolved BCP) solution in a good solvent for both blocks. This is a protracted multistep process that leads to very low final BCP concentrations (< 1% w/w solids) that hinder commercial scale up. In

addition, access to non-spherical micelles is a major challenge as these generally only exist in a very restricted region of compositional phase space and are often contaminated by other morphologies. Moreover, where non-spherical nanoparticle morphologies can be accessed, the resulting samples are polydisperse, and contain micelles that vary in size. The formation of monodisperse micelles with precise control of their dimensions and therefore properties cannot be achieved[8].

Polymerisation-Induced Self-Assembly (PISA) represents an emerging route of rapidly growing interest for the formation of BCP core-shell nanostructures in solution whereby polymerisation and self-assembly of amphiphilic diblock copolymers occur *in situ*[9-11]. Significantly, PISA can be carried out at high weight percent of solids (ca. 10 - 50% w/w solids) in either organic or aqueous media and is increasingly being flagged as a potential scale-up process for the industrial synthesis of BCP micelles. In principle, PISA can be carried out using any living/controlled polymerisation method in which spontaneous chain transfer and chain termination are minimised[12-15], however, the majority of examples currently use reversible addition−fragmentation chain transfer (RAFT) polymerisation[16-23]. In a typical PISA synthesis the first step involves preparation of a macromolecular initiator that will ultimately form the corona-forming block. In the second step, the macroinitiator is dispersed in the presence of a second monomer and a radical initiator in a selective solvent. As the degree of polymerisation (DP_n) of the second insoluble core-forming block increases, self-assembly is induced. This process can often be accompanied by a change in micellar morphology, most typically from spheres, to cylindrical (or worm-like) micelles, through to platelets or vesicles[24-28]. Access to cylindrical micelles is particularly desirable for applications in 'smart thickening' and composite reinforcement, and for uses as drug delivery vehicles with long circulation times and as nanowires. Recent advances using crystallisable BCP amphiphiles, as well as crystallisable homopolymers, include the formation of highly concentrated dispersions of cylinders from BCP containing liquid crystalline cholesteryl moieties[29] and semicrystalline poly(stearyl methacrylate) cores[30], elongated micelles with crystalline polythiophene[31-32] and polyacetylene[33] core-forming blocks, and nanoplatelets from polyethylene homopolymer[34]. However, for the overwhelming majority of PISA formulations the cylindrical morphology occupies only a small region of phase space. In addition, the length control of cylindrical micelles using PISA methods has not yet been achieved and has been described as a formidable technical challenge[9].

Crystallisation-Driven Self-Assembly (CDSA) of BCPs with a crystallisable core-forming block is an alternative route for the preparation non-spherical core-shell nanostructures that provides excellent levels of dimensional control[35]. Unlike their all-amorphous analogues, BCPs with a crystalline core-forming block generally prefer to form micelles with a low mean curvature of the

core-corona interface when dispersed in a selective solvent. CDSA has been employed for a variety of amphiphiles where crystalline polymer segments or planar π-stacking species participate in core formation, including biodegradable[36-38], bioinert[39] and π-conjugated materials[40-44]. However, the most extensively studied core-forming block is poly(ferrocenyldimethylsilane) (PFDMS)[45]. Significantly, in the case of cylinder formation, the termini of the crystalline PFDMS micelle cores remain active to the addition of unimer and growth occurs via epitaxy[46]. Using small seed micelles (prepared by the sonication of longer cylindrical micelles) as nucleation sites, cylinders of controlled length and with narrow length dispersities can be prepared by varying the unimer-to-seed micelle ratio, a process analogous to a living covalent polymerisation of molecular monomers that has been termed 'living CDSA'[35]. Living CDSA has been utilised in the preparation of 1D cylindrical micelles[35], 2D lenticular and rectangular platelet micelles[47,48] and multi-compartment block comicelles[49] with controlled dimensions and spatially defined functionality. However, despite the exceptional control living CDSA offers, multiple step post-polymerisation solution processing is carried out on a small scale with dilute concentrations of micelles (typically < 0.5% w/w solids). Inspired by the scale-up opportunities and commercial viability of PISA on one hand, and the unprecedented levels of control displayed by living CDSA on the other, we report the successful combination of these two methods with a view to forming monodisperse, 1D cylindrical micelles of controlled length at high weight percentages of solids. We term this process Polymerisation-Induced Crystallisation-Driven Self-Assembly (PI-CDSA).

Results and Discussion

In this proof of concept work we focused on the synthesis and self-assembly of amphiphilic PFDMS BCPs formed by sequential living anionic polymerisation with no isolation and purification steps. The PI-CDSA process necessitated the initial formation of a corona-forming block that was well-controlled under living anionic conditions in a solvent medium that fully solvated this segment. A second requirement was that the medium was increasingly selective for the corona-forming block as the degree of polymerisation of PFDMS increased during the subsequent step. To satisfy these criteria we selected polyisoprene-*b*-poly(ferrocenyldimethylsilane) (PIP-*b*-PFDMS) BCPs in a THF/n-hexanes solvent mixture, as THF is a good solvent for both PIP and PFDMS and n-hexanes is a selective solvent that is good for PIP, but poor for PFDMS. The self-assembly of PIP-*b*-PFDMS BCPs in n-hexanes is well understood[35,50] and it was therefore anticipated that at a threshold degree of polymerisation, the PFDMS block would become insoluble, and PI-CDSA would occur (Fig. 1 and Supplementary Fig. 1a). Initial experiments were carried out at ca. 10% w/w solids, well within

the accepted regime of PISA, but at far greater concentrations than typical CDSA processes for PFDMS BCPs (< 0.5% w/w solids). Monodisperse samples of anion-terminated PIP were prepared by living anionic polymerisation in 100% THF yielding PIP_{58}, PIP_{193} and PIP_{389} (where subscripts denote the degree of polymerisation). Small aliquots of the PIP homopolymers were removed for characterisation by matrix assisted laser desorption/ionisation – time of flight (MALDI-TOF) mass spectrometry and gel permeation chromatography (GPC) (Supplementary Table 1) before the addition of dimethylsila[1]ferrocenophane monomer in n-hexanes to the living PIP solution in THF to give an overall solvent composition of 10% v/v, 20% v/v and 40% v/v THF in a majority n-hexanes solvent mixture. Previous investigations into the influence of block ratio upon the self-assembly of PFDMS BCPs have shown that 2D platelet micelles are formed when the block ratio between the two blocks is close to 1:1 and 1D cylindrical micelles over a wide range of block ratios between 5:1 and 20:1[50,51]. A series of PIP-*b*-PFDMS BCPs were targeted with block ratios of 1:1, 5:1 and 10:1 in varying THF/n-hexanes solvent ratios (Supplementary Table 2). After 1 h the polymerisations were quenched with 4-tert-butylphenol (TBP) and small aliquots of the solutions spotted onto carbon-coated copper grids for analysis by Transmission Electron Microscopy (TEM).

TEM revealed the formation of micelles for all of the PIP-*b*-PFDMS BCPs at 10% v/v and 20% v/v THF/n-hexanes. For PIP-*b*-PFDMS BCPs with a targeted block ratio = ca. 1:1 in 10% v/v and 20% v/v THF/n-hexanes 2D lenticular platelet micelles were formed (Fig. 2a, d; see also Supplementary Fig. 2, 3, 4 and Supplementary Table 3). At targeted block ratios of ca. 5:1 and 10:1 in 10% v/v and 20% v/v THF/n-hexanes cylindrical micelles were formed (Fig. 2b, e and 2c, f; see also Supplementary Fig. 2 and Supplementary Table 3). These morphologies are consistent with those observed for the self-assembly of PFDMS BCPs performed at significantly lower concentrations[50]. At 40% v/v THF/n-hexanes, no micelles were observed by TEM at any block ratio, however a phase-separated film derived from unimer was obtained (Supplementary Fig. 5). For comparison, a PIP-*b*-PFMPS (PFMPS = poly(ferrocenylmethylphenylsilane)) BCP with a targeted block ratio of 5:1 containing a PFMPS block that does not crystallise was also prepared. For this material spherical micelles were observed by TEM (Supplementary Fig. 6) underscoring the key role of core crystallisation in the self-assembly process for the PFDMS BCPs. Indeed, the crystallinity of the PFDMS core-forming block of the cylindrical micelles prepared via PI-CDSA was confirmed by in situ solution-phase wide-angle X-ray scattering (WAXS). The WAXS pattern for the cylindrical micelles displayed a sharp peak with d-spacing of 6.3 Å which is characteristic of crystalline PFDMS, (Supplementary Fig. 7) with a crystallite size of 12.2 nm based on the peak width (Supplementary Table 4). The latter value corresponds approximately to the width of the micelles[52].

These results demonstrated that a PI-CDSA approach for the formation of non-spherical but polydisperse micelles with the predicted morphologies at high percentage solids was possible under these conditions. Furthermore, the versatility of the PI-CDSA approach was demonstrated using a different corona-forming block, namely poly(4-tert-butylstyrene) (PtBS), to prepare polydisperse cylindrical micelles of $PtBS_{256}$-*b*-$PFDMS_{51}$ (see Supplementary Information page 4 and Supplementary Fig. 8).

In order to provide more detailed insight into the PI-CDSA process and, specifically, to determine if polymerisation and self-assembly occur simultaneously, we exploited the propensity for PFDMS BCPs with a 1:1 block ratio to form platelets as a method to determine the extent of self-assembly and the degree of polymerisation of the PFDMS block at a series of time points. The PI-CDSA of a targeted PIP_{44}-*b*-$PFDMS_{57}$ BCP (block ratio = 1.0:1.3) was carried out as described above with aliquots removed at a series of time points following the addition of the dimethylsila[1]ferrocenophane monomer for characterisation by GPC and ^{1}H NMR (Supplementary Table 5 and Supplementary Fig. 9) and TEM (Supplementary Fig. 10 and 11). Aliquots collected at time points up to and including 2 min displayed no micelles by TEM with only film detected and a PIP_{44}-*b*-PFDMS BCP with a PFDMS DP_n = 17 at t = 2 min. At t = 5 min, ill-defined aggregates with cylindrical protrusions as well as film were observed by TEM with a PFDMS DP_n = 35. At t = 10 and 20 min platelet and cylindrical micelles were observed with background film also present and a PFDMS DP_n = 44 (t =10 min) and PFDMS DP_n = 50 (t = 20 min), respectively. At t = 40 min and a PFDMS DP_n = 57 a morphological transition had occurred with virtually no cylindrical micelles present. Instead, large aggregates of platelet micelles were detected with no background film present on the TEM grid. We conclude from these results that polymerisation and self-assembly occur almost simultaneously throughout the PI-CDSA process under the conditions used with a morphological change from cylinders at low DP_n of the PFDMS block to platelets as the block ratio moves towards 1:1, as in this case. Furthermore, these results demonstrate that complete conversion of the sila[1]dimethylferrocenophane monomer and self-assembly to form platelet micelles both take place within ca. 40 mins.

The ability to prepare BCP nanostructures by PI-CDSA at concentrations potentially commensurate with manufacturing processes is an important advance. In an attempt to extend the limit of our system even further, we attempted PI-CDSA at 25% w/w solids of a PIP_{174}-*b*-$PFDMS_{39}$ BCP (block ratio 4.5:1.0, Supplementary Table 6). PI-CDSA was carried out as previously described at 20% v/v THF/n-hexanes. Following addition of the dimethylsila[1]ferrocenophane monomer to the living PIP,

the resulting solution became viscous within 10 min and then rapidly turned into a gel. Remarkably, TEM analysis of diluted solutions of the resulting gel revealed it to be comprised of a densely packed, multi-micron long cylindrical micelles (Fig. 3).

Having established that PI-CDSA can be used to prepare polydisperse cylindrical micelles over a range of block ratios and up to 25% w/w solids, we aimed to also incorporate the seeded growth approach employed for solution-based living CDSA to prepare monodisperse cylindrical micelles with length control. Living CDSA utilises small seed micelles formed from the ultrasonication of long, polydisperse cylindrical micelles as initiators[35]. These were prepared by the ultrasonication of polydisperse PIP_{168}-*b*-$PFDMS_{24}$ BCP (block ratio 7.0:1.0) to yield seed micelles (number averaged length L_n = 64, length dispersity, L_w/L_n = 1.14, L_w = weight averaged length, Supplementary Fig. 12) at 30 mg/mL. The small seed micelles were added to the stirred solution of dimethylsila[1]ferrocenophane in n-hexanes followed by the addition of the solution of living PIP in THF to give an overall solvent composition of 10% v/v THF/n-hexanes (Fig. 4 and Supplementary Fig. 1b). To investigate this approach a range of monomer-to-seed ratios were chosen (3:1, 6:1, 9:1, 12:1, 15:1, 18:1 and 21:1) to explore if it would be possible to replicate the living CDSA observed for the solution self-assembly of PFDMS-based BCPs to generate monodisperse, 1D micelles of controlled length at 10% w/w solids. All solutions became turbid within 15 min of the addition of living PIP. Analysis of the resulting nanoparticles by TEM demonstrated a linear relationship between cylindrical micelle contour length and the monomer-to-seed ratio (Fig. 4b-k, Supplementary Fig. 12-15, and Table 1). Low dispersity samples of cylindrical micelles with lengths from 500 nm to 3 μm were successfully prepared using this approach (for the case of L_n = 560 nm see Atomic Force Microscopy (AFM) Images in Fig. 5 and Supplementary Fig. 16). Significantly, this living PI-CDSA approach demonstrates the ability to rapidly prepare monodisperse cylindrical micelles (in < 5 h starting from initiation of isoprene - this compares to days for the usual sequential polymerisation, isolation, and solution processing method). In addition, ^{1}H NMR and GPC analysis showed the composition of the BCPs for each micelle length to be virtually identical (Table 1, Supplementary Table 7 and Supplementary Fig. 17) indicating the reproducibility of this living PI-CDSA process. These experiments demonstrate the first preparation of monodisperse cylindrical micelles via a PISA platform at 10% w/w solids. Furthermore, although the concentration limit for successful living PI-CDSA has not yet been determined, we have also been able to prepare near monodisperse micelles at 22% w/w solids (see Supplementary Information and Supplementary Fig. 18).

Conclusions

In summary, we demonstrate the rapid and convenient preparation of non-spherical micelles at concentrations up to 25% w/w solids by the synchronous coupling of established PISA and CDSA protocols, in a process we have termed PI-CDSA. In addition, the living CDSA approach can be applied, allowing access to monodisperse cylindrical micelles of controlled length. In this proof of concept work we have focussed on the use of anionic polymerisation and BCPs based on PFDMS. Clearly, PI-CDSA should be extendable to other BCPs with crystalline core-forming blocks that can be prepared by this well-developed polymerisation protocol. More significantly, the success of PI-CDSA even under the stringent conditions required for living anionic polymerisations suggests the potentially general applicability of this approach to other crystallisable BCPs that can be prepared by other living/controlled polymerisation methods[12-15]. Scalable access to samples of monodisperse cylinders of controlled length based on different BCP chemistries via a one-pot procedure from monomer precursors using the living PI-CDSA method as illustrated here is expected to facilitate tailoring properties for a range of applications in fields that range from nanomedicine to composite toughening.

Methods

General Experimental Considerations

Anionic polymerisations were carried out in a nitrogen atmosphere glovebox. All other manipulations were carried out under an open atmosphere unless otherwise stated. All reagents were purchased from Sigma-Aldrich unless otherwise stated. Dimethylsila[1]ferrocenophane monomer was prepared from ferrocene, N,N,N',N'-tetramethylethylenediamine (TMEDA), *n*-Butyllithium (*n*-BuLi) and dichlorodimethylsilane[53]. Monomer purifications were performed under an atmosphere of purified N_2. Isoprene and 4-tert-butylstyrene monomers were purchased from Sigma Aldrich and dried over CaH_2 and distilled under reduced pressure followed by a second distillation from n-BuLi. THF was distilled from Na/benzophenone immediately before use. n-Hexanes was purified using Anhydrous Engineering double alumina and alumina/copper catalyst drying columns. ^1H and NMR spectra were recorded using Varian VNMR 400 MHz spectrometers.

Polymer Characterization

Gel permeation chromatography was carried out using a Viscotek VE 2001 Triple-Detector Gel Permeation Chromatograph equipped with an automatic sampler, a pump, an injector, an inline

degasser, and a column oven (30 °C). The elution columns consist of styrene/divinylbenzene gels with pore sizes between 500 Å and 100,000 Å. Detection was conducted by means of a VE 3580 refractometer, a four-capillary differential viscometer, and 90° and low angle (7°) laser light (λ_0= 670 nm) scattering detectors, VE 3210 & VE 270. THF (Fisher) was used as the eluent, with a flow rate of 1.0 mL/min. Samples were dissolved in the eluent (2 mg/mL) and filtered with a Ministart SRP 15 filter (polytetrafluoroethylene membrane of 0.45 μm pore size) before analysis. The calibration was conducted using a PolyCAL^{TM} polystyrene standard (PS115K) from Viscotek. Matrix-assisted laser desorption/ionisation time of flight (MALDI-TOF) mass spectrometry measurements were performed using a Bruker Ultraflextreme running in linear mode. Samples were prepared using a trans-2-[3-(4-tert-butylphenyl)-2-methyl-2-propenylidene]malononitrile matrix (20 mg/mL in THF), silver trifluoroacetate (10 mg/mL) and the polymer sample (2 mg/mL in THF), mixed in a 10:1:1 (v/v/v) ratio. Approximately 1 μL of the mixed solution was deposited onto a MALDI sample plate and allowed to dry in air. The molecular weights and degrees of polymerisation for the diblock copolymers were then determined by combining the molecular weight M_n of the first block from MALDI-TOF measurements with the block ratio of the diblock copolymer obtained by integrating the ^{1}H NMR spectroscopic signal intensities of the respective blocks.

Transmission electron microscopy (TEM)

Copper grids from Agar Scientific, mesh 400, were coated with a carbon film. Carbon coating was done using an Agar TEM Turbo Carbon Coater where carbon was sputtered onto mica sheets before deposition on the copper grids via flotation on water. Bright field TEM micrographs were obtained on a JEOL1200EX II microscope operating at 120 kV and equipped with an SIS MegaViewIII digital camera or JEOL 1400 microscope operating at 120 kV and equipped with a Gatan digital camera. The samples for electron microscopy were prepared by drop casting one drop (*ca.* 10 μL) of the micelle colloidal solution onto a carbon coated copper grid.

Atomic Force Microscopy (AFM)

AFM analyses were performed in ambient conditions using a Bruker Multimode VIII atomic force microscope equipped with a ScanAsyst-HR fast scanning module and a ScanAsyst-Air-HR probe (tip radius, 2 nm), utilising peak force feedback control. The samples prepared for TEM analysis were also used for imaging by AFM (see above).

Manual tracing of the micelle images

Micelle contour lengths were estimated from the TEM images manually using the ImageJ software package developed at the US National Institute of Health. For the statistical length analyses, 200 objects were processed to determine the contour length of the data set. Each TEM image was analysed completely, *i.e.* every micelle in each image was counted in order to reduce subjectivity. From this data, histogram were constructed and values of the mean contour length L_n, weighted contour length L_w, standard deviation σ and polydispersity index (*PDI*) were estimated using the following equations where N is the sample size:

$$L_n = \frac{\sum_{i=1}^{n} N_i L_i}{\sum_{i=1}^{n} N_i}$$

$$L_w = \frac{\sum_{i=1}^{n} N_i L_i^2}{\sum_{i=1}^{n} N_i L_i}$$

$$\sigma = \sqrt{\frac{1}{N}\sum_{i=1}^{n}(x_i - \mu)^2}$$

$$PDI = \frac{L_w}{L_n}$$

Data Availability

All data is available from https://data.bris.ac.uk/data or by request from the corresponding author.

References

1. Hayward, R. C. & Pochan, D. J. Tailored Assemblies of Block Copolymers in Solution: It Is All about the Process. *Macromolecules* **43,** 3577–3584 (2010).

2. Gröschel, A. H. *et al.* Guided hierarchical co-assembly of soft patchy nanoparticles. *Nature* **7**, 11841-11876 (2013).

3. Blanazs, A., Armes, S. P. & Ryan, A. J. Self-assembled block copolymer aggregates: From micelles to vesicles and their biological applications. *Macromol. Rapid Commun.* **30,** 267–277 (2009).

4. Schacher, F. H., Rupar, P. A. & Manners, I. Functional Block Copolymers: Nanostructured Materials with Emerging Applications. *Angew. Chem. Int. Ed.* **51,** 7898–7921 (2012).

5. Elsabahy, M. & Wooley, K. L. Design of polymeric nanoparticles for biomedical delivery applications. *Chem. Soc. Rev.* **41,** 2545–2561 (2012).

6. Gröschel, A. H. & Müller, A. H. E. Self-assembly concepts for multicompartment nanostructures. *Nanoscale* **7,** 11841–11876 (2015).

7. Ge, Z. & Liu, S. Functional block copolymer assemblies responsive to tumor and intracellular microenvironments for site-specific drug delivery and enhanced imaging performance. *Chem. Soc. Rev.* **42,** 7289-7325 (2013).

8. Lodge, T. P. Block Copolymers: Past Successes and Future Challenges. *Macromol. Chem. Phys.* **204,** 265–273 (2003).

9. Canning, S. L., Smith, G. N. & Armes, S. P. A Critical Appraisal of RAFT-Mediated Polymerization-Induced Self-Assembly. *Macromolecules* **49,** 1985–2001 (2016).

10. Derry, M. J., Fielding, L. A. & Armes, S. P. Polymerization-induced self-assembly of block copolymer nanoparticles via RAFT non-aqueous dispersion polymerization. *Prog. Polym. Sci.* **52,** 1–18 (2016).

11. Warren, N. J. & Armes, S. P. Polymerization-Induced Self-Assembly of Block Copolymer Nano-objects via RAFT Aqueous Dispersion Polymerization. *J. Am. Chem. Soc.* **136,** 10174–10185 (2014).

12. Hawker, C. J., Bosman, A. W. & Harth, E. New Polymer Synthesis by Nitroxide Mediated Living Radical Polymerizations. *Chem. Rev.* **101,** 3661–3688 (2001).

13. Moad, G., Rizzardo, E. & Thang, S. H. Living Radical Polymerization by the RAFT Process—A First Update. *Aust. J. Chem.* **59,** 669-692 (2006).

14. Kamigaito, M., Ando, T. & Sawamoto, M. Metal-Catalyzed Living Radical Polymerization. *Chem. Rev.* **101,** 3689–3746 (2001).

15. Matyjaszewski, K. & Xia, J. Atom Transfer Radical Polymerization. *Chem. Rev.* **101,** 2921–2990 (2001).

16. Jia, Z., Bobrin, V. A., Truong, N. P., Gillard, M. & Monteiro, M. J. Multifunctional Nanoworms and Nanorods through a One-Step Aqueous Dispersion Polymerization. *J. Am. Chem. Soc.* **136,** 5824–5827 (2014).

17. Kim, K. H., Kim, J. & Jo, W. H. Preparation of hydrogel nanoparticles by atom transfer radical polymerization of N-isopropylacrylamide in aqueous media using PEG macro-initiator. *Polymer* **46,** 2836–2840 (2005).

18. Sugihara, S., Sugihara (nee Nishikawa), K., Armes, S. P., Ahmad, H. & Lewis, A. L. Synthesis of Biomimetic Poly(2-(methacryloyloxy)ethyl phosphorylcholine) Nanolatexes via Atom Transfer Radical Dispersion Polymerization in Alcohol/Water Mixtures. *Macromolecules* **43,** 6321–6329 (2010).

19. Delaittre, G., Nicolas, J., Lefay, C., Save, M. & Charleux, B. Surfactant-free synthesis of amphiphilic diblock copolymer nanoparticles via nitroxide-mediated emulsion polymerization. *Chem. Commun.* **5,** 614–616 (2005).

20. An, Z. *et al.* Facile RAFT Precipitation Polymerization for the Microwave-Assisted Synthesis of Well-Defined, Double Hydrophilic Block Copolymers and Nanostructured Hydrogels. *J. Am. Chem. Soc.* **129,** 14493–14499 (2007).

21. Delaittre, G., Save, M. & Charleux, B. Nitroxide-Mediated Aqueous Dispersion Polymerization: From Water-Soluble Macroalkoxyamine to Thermosensitive Nanogels. *Macromol. Rapid Commun.* **28,** 1528–1533 (2007).

22. Liu, G., Qiu, Q., Shen, W. & An, Z. Aqueous Dispersion Polymerization of 2-Methoxyethyl Acrylate for the Synthesis of Biocompatible Nanoparticles Using a Hydrophilic RAFT Polymer and a Redox Initiator. *Macromolecules* **44,** 5237–5245 (2011).

23. Sun, J.-T., Hong, C.-Y. & Pan, C.-Y. Formation of the block copolymer aggregates via polymerization-induced self-assembly and reorganization. *Soft Matter* **8,** 7753 (2012).

24. He, W.-D., Sun, X.-L., Wan, W.-M. & Pan, C.-Y. Multiple Morphologies of PAA-*b*-PSt Assemblies throughout RAFT Dispersion Polymerization of Styrene with PAA Macro-CTA. *Macromolecules* **44,** 3358–3365 (2011).

25. Cai, W., Wan, W., Hong, C.-Y., Huang, C.-Q. & Pan, C.-Y. Morphology transitions in RAFT polymerization. *Soft Matter* **6,** 5554 (2010).

26. Zhang, X. *et al.* Well-Defined Amphiphilic Block Copolymers and Nano-objects Formed in Situ via RAFT-Mediated Aqueous Emulsion Polymerization. *Macromolecules* **44,** 4149–4158 (2011).

27. Huang, C.-Q. & Pan, C.-Y. Direct preparation of vesicles from one-pot RAFT dispersion polymerization. *Polymer* **51,** 5115–5121 (2010).

28. Yang, P., Ratcliffe, L. P. D. & Armes, S. P. Efficient Synthesis of Poly(methacrylic acid)-*block*-Poly(styrene-*alt*-N-phenylmaleimide) Diblock Copolymer Lamellae Using RAFT Dispersion Polymerization. *Macromolecules* **46,** 8545–8556 (2013).

29. Zhang, X. *et al.* Amphiphilic liquid-crystal block copolymer nanofibers via RAFT-mediated dispersion polymerization. *Soft Matter* **8,** 1130–1141 (2012).

30. Semsarilar, M., Penfold, N. J. W., Jones, E. R. & Armes, S. P. Semi-crystalline diblock copolymer nano-objects prepared via RAFT alcoholic dispersion polymerization of stearyl methacrylate. *Polym. Chem.* **6,** 1751–1757 (2015).

31. Lee, I. H. *et al.* Nanostar and Nanonetwork Crystals Fabricated by in Situ Nanoparticlization of Fully Conjugated Polythiophene Diblock Copolymers. *J. Am. Chem. Soc.* **135,** 17695–17698 (2013).

32. Lee, I. H., Amaladass, P. & Choi, T. L. One-pot synthesis of nanocaterpillar structures via in situ nanoparticlization of fully conjugated poly(p-phenylene)-block-polythiophene. *Chem. Commun.* **50,** 7945-7948 (2014).

33. Yoon, K.-Y. *et al.* One-Pot in Situ Fabrication of Stable Nanocaterpillars Directly from Polyacetylene Diblock Copolymers Synthesized by Mild Ring-Opening Metathesis Polymerization. *J. Am. Chem. Soc.* **134,** 14291–14294 (2012).

34. Weber, C. H. M. *et al.* Single lamella nanoparticles of polyethylene. *Nano Lett.* **7,** 2024-2029 (2007).

35. Gilroy, J. B. *et al.* Monodisperse cylindrical micelles by crystallization-driven living self-assembly. *Nat. Chem.* **2,** 566–570 (2010).

36. Yang, J.-X. *et al.* Hydrogen-Bonding-Mediated Fragmentation and Reversible Self-assembly of Crystalline Micelles of Block Copolymer. *Macromolecules* **49,** 367–372 (2016).

37. Petzetakis, N., Dove, A. P. & O'Reilly, R. K. Cylindrical micelles from the living crystallization-driven self-assembly of poly(lactide)-containing block copolymers. *Chem. Sci.* **2,** 955–960 (2011).

38. Sun, L. *et al.* Structural reorganization of cylindrical nanoparticles triggered by polylactide stereocomplexation. *Nat. Commun.* **5,** 5746 (2014).

39. Schmelz, J., Schedl, A. E., Steinlein, C., Manners, I. & Schmalz, H. Length control and block-type architectures in worm-like micelles with polyethylene cores. *J. Am. Chem. Soc.* **134,** 14217–14225 (2012).

40. Ogi, S., Stepanenko, V., Sugiyasu, K., Takeuchi, M. & Würthner, F. Mechanism of Self-Assembly Process and Seeded Supramolecular Polymerization of Perylene Bisimide Organogelator. *J. Am. Chem. Soc.* **137,** 3300–3307 (2015).

41. Zhang, W. *et al.* Supramolecular Linear Heterojunction Composed of Graphite-Like Semiconducting Nanotubular Segments. *Science* **334,** 340–343 (2011).

42. Ogi, S., Sugiyasu, K., Manna, S., Samitsu, S. & Takeuchi, M. Living supramolecular polymerization realized through a biomimetic approach. *Nat. Chem.* **6,** 188–195 (2014).

43. Qian, J. *et al.* Uniform, high aspect ratio fiber-like micelles and block co-micelles with a crystalline π-conjugated polythiophene core by self-seeding. *J. Am. Chem. Soc.* **136,** 4121–4124 (2014).

44. Robinson, M. E. *et al.* Length control of supramolecular polymeric nanofibers based on stacked planar platinum(II) complexes by seeded-growth. *Chem. Commun.* **51,** 15921–15924 (2015).

45. Hailes, R. L. N., Oliver, A. M., Gwyther, J., Whittell, G. R. & Manners, I. Polyferrocenylsilanes: synthesis, properties, and applications. *Chem. Soc. Rev.* **45,** 5358-5407 (2016).

46. Wang, X. *et al.* Cylindrical Block Copolymer Micelles and Co-Micelles of Controlled Length and Architecture. *Science* **317,** 644–647 (2007).

47. Hudson, Z. M. *et al.* Tailored hierarchical micelle architectures using living crystallization-driven self-assembly in two dimensions. *Nat. Chem.* **6,** 893–898 (2014).

48. Qiu, H. *et al.* Uniform patchy and hollow rectangular platelet micelles from crystallizable polymer blends. *Science* **352,** 697–701 (2016).

49. Hudson, Z. M., Lunn, D. J., Winnik, M. A. & Manners, I. Colour-tunable fluorescent multiblock micelles. *Nat. Commun.* **5,** 3372 (2014).

50. Cao, L., Manners, I. & Winnik, M. A. Influence of the interplay of crystallization and chain stretching on micellar morphologies: Solution self-assembly of coil-crystalline poly(isoprene-block-ferrocenylsilane). *Macromolecules* **35,** 8258–8260 (2002).

51. Massey, J. A. *et al.* Self-assembly of organometallic block copolymers: The role of crystallinity of the core-forming polyferrocene block in the micellar morphologies formed by poly(ferrocenylsilane-*b*-dimethylsiloxane) in n-alkane solvents. *J. Am. Chem. Soc.* **122,** 11577–11584 (2000).

52. Gilroy, J. B. *et al.* Probing the Structure of the Crystalline Core of Field-Aligned, Monodisperse, Cylindrical Polyisoprene-block-Polyferrocenylsilane Micelles in Solution Using Synchrotron Small-and Wide-Angle X-ray Scattering. *J. Am. Chem. Soc.* **133,** 17056–17062 (2011).

53. Ni, Y., Rulkens, R. & Manners, I. Transition Metal-Based Polymers with Controlled Architectures: Well-Defined Poly(ferrocenylsilane) Homopolymers and Multiblock Copolymers via the Living Anionic Ring-Opening Polymerization of Silicon-Bridged [1]Ferrocenophanes. *J. Am. Chem. Soc.* **118,** 4102–4114 (1996).

Supplementary Information

Supplementary Information is linked to the online version of the paper at www.nature.com/nature.

Acknowledgements

C.E.B. thanks the Bristol Chemical Synthesis Centre for Doctoral Training, funded by the Engineering and Physical Sciences Research Council (EPSRC) for a Ph.D. studentship. J. G. thanks the EPSRC for funding. D.W.H. thanks the EPSRC-funded Bristol Centre for Functional Nanomaterials doctoral training grant [EP/G036780/1]. Correspondence and requests for materials should be addressed to I.M. (ian.manners@bristol.ac.uk).

Author Contributions

C. E. B. and J. G. contributed equally to this work. C. E. B. and J. G. devised the project and carried out the experiments. R. L. H performed AFM experiments. D. W. H. performed the scattering experiments. C.E.B., J. G. and I.M. wrote the manuscript with input from D. W. H. The project was supervised by I.M.

Competing Financial Interests

The authors declare no competing financial interests.

Figure Captions

Figure 1: Schematic representations of the preparation of polydisperse PIP-*b*-PFDMS cylindrical micelles. a) Preparation of PIP-*b*-PFDMS diblock copolymer by sequential living anionic polymerisation followed by b) multi-step post-polymerisation solution processing of the PIP-*b*-PFDMS diblock copolymers using CDSA protocols. By combining established PISA and CDSA techniques PIP-*b*-PFDMS cylindrical micelles can be rapidly prepared (< 5 h starting from initiation of isoprene compared with days for separate polymerisation and processing methods) at high percentage solids (up to 25% w/w solids) by PI-CDSA. TBP = 4-tert-butylphenol was used as quenching agent. PIP = 3,4-polyisoprene (~60%, shown in a)), 1,2-polyisoprene (~30%) and trans-1,4-polyisoprene (~10%).[50]

Figure 2: PI-CDSA (at 10% w/w solids) of PIP-*b*-PFDMS at 10% v/v THF/n-hexanes with varying block ratios. a-f) Bright field TEM micrographs of dried polydisperse micelles of PIP-*b*-PFDMS with varying block ratios prepared by PI-CDSA at 10% w/w solids diluted to 1 mg/mL for TEM imaging. Lenticular platelet micelles were formed for PIP-*b*-PFDMS BCPs with a targeted block ratio = ca. 1:1 a) and d) and cylindrical micelles were formed for block ratios = ca. 5:1 b) and e) and 10:1 c) and f). Scale bars: a-c) = 1 μm d-f) = 500 nm.

Figure 3: PI-CDSA (at 25% w/w solids) of PIP-*b*-PFDMS with a block ratio = 4.5:1.0 in 20% v/v THF/n-hexanes. a, b) Images of sample vial containing a micellar gel. c, d and e) Bright field TEM micrographs of dried polydisperse, densely packed, multi-micron long cylindrical micelles of PIP-*b*-PFDMS diluted to 10 mg/mL (c and d) and 1 mg/mL (e) in 20% v/v THF/n-hexanes for TEM imaging. Scale bars: c, e) = 1 μm d) = 500 nm.

Figure 4: a) Schematic representation of the preparation of near monodisperse PIP-*b*-PFDMS cylindrical micelles via living PI-CDSA. TBP = 4-tert-butylphenol was used as a quenching agent. PI-CDSA seeded growth of PIP-*b*-PFDMS cylindrical micelles was carried out at 10% w/w solids in 10% v/v THF/n-hexanes. b–i) High magnification bright field TEM micrographs of dried near monodisperse cylindrical micelles of PIP-*b*-PFDMS prepared by living PI-CDSA and diluted to 1 mg/mL. b) Small seed micelles prepared by the ultra-sonication of long polydisperse micelles. Monomer-to-seed ratios of c) 3:1, d) 6:1, e) 9:1, f) 12:1, g) 15:1, h) 18:1, i) 21:1. j) Plot illustrating the linear dependence of the micelle contour length on the monomer-to-seed ratio (the latter is proportional to the unimer-to-seed ratio used in conventional living CDSA plots[35]). Error bars, standard deviation of measured micelle contour lengths. k) Histogram of the contour length

distribution of small seed micelles (y axis-scale reduced by 2) and selected samples with monomer-to-seed ratios of 3:1, 9:1, 15:1, 21:1 k). For other ratios see Supplementary Fig. 15. Scale bars = 1000 nm, inset scale bar = 200 nm.

Figure 5: AFM images of PIP-*b*-PFDMS cylindrical micelles (L_n = 560 nm, PDI = 1.04) prepared at 10% w/w solids by living PI-CDSA in 10% v/v THF/n-hexanes. a) Low magnification AFM height profile images of dried near monodisperse cylindrical micelles of PIP-*b*-PFDMS. b) High magnification AFM height profile images illustrating the high density of the near monodisperse micelles prepared by this method. Scale bars a) 2000 nm, b) = 500 nm

Table 1: Contour length data for the cylindrical micelles and BCP composition for living PI-CDSA at 10% w/w solids[a]

monomer/ seed ratio	seeds	3:1	6:1	9:1	12:1	15:1	18:1	21:1
L_n (nm)	64	560	931	1407	1597	2041	2433	2862
L_w (nm)	73	580	957	1433	1617	2070	2456	2889
PDI	1.14	1.04	1.03	1.02	1.01	1.01	1.01	1.01
σ (nm)	24	107	158	191	180	245	236	283
BCP	PIP_{168}-*b*-PFS_{24}	PIP_{154}-*b*-PFS_{29}	PIP_{154}-*b*-PFS_{28}	PIP_{154}-*b*-PFS_{29}	PIP_{154}-*b*-PFS_{29}	PIP_{154}-*b*-PFS_{29}	PIP_{154}-*b*-PFS_{29}	PIP_{154}-*b*-PFS_{29}
Block ratio	7:1	5.3:1	5.5:1	5.3:1	5.3:1	5.3:1	5.3:1	5.3:1

[a]For each sample 200 micelles were counted for the statistical data

Table of Contents Summary

Polymerisation-Induced Crystallisation-Driven Self-Assembly (PI-CDSA), a scalable "one-pot" block copolymer synthesis-solution processing protocol, is described. This approach offers facile access to non-spherical micelle morphologies such as cylinders and platelets. Moreover, in the presence of small seed micelles dimensional control is possible. This is illustrated by the formation of near-uniform samples of cylindrical micelles with lengths up to several microns.

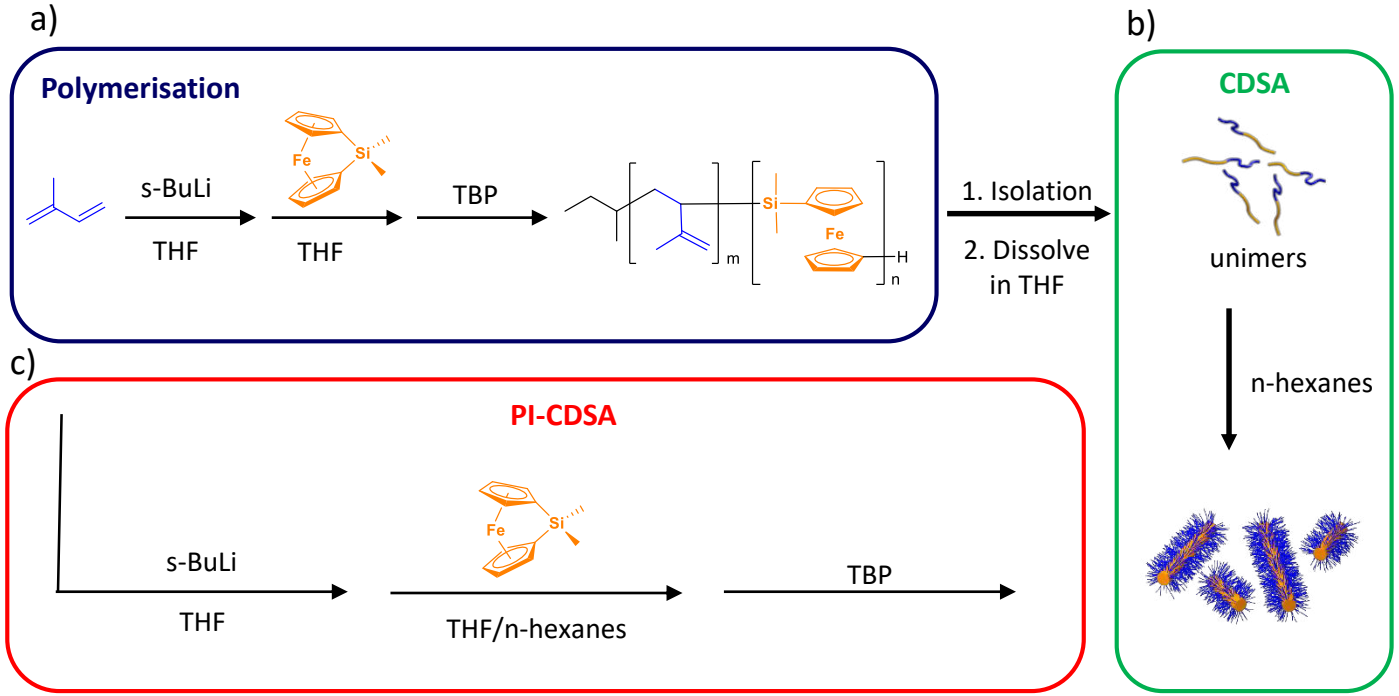
a)
Polymerisation
s-BuLi
THF
THF
TBP
Fe
Si
m
n
H
1. Isolation
2. Dissolve in THF
b)
CDSA
unimers
n-hexanes
c)
PI-CDSA
s-BuLi
THF
THF/n-hexanes
TBP

1:1 = 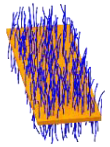

5:1 = 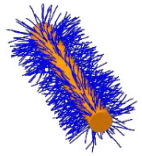

10:1 = 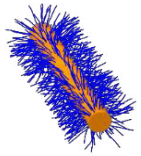

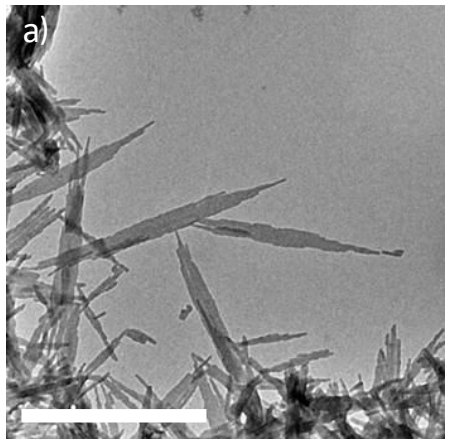

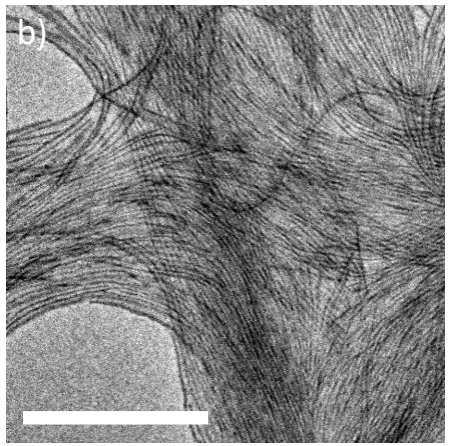

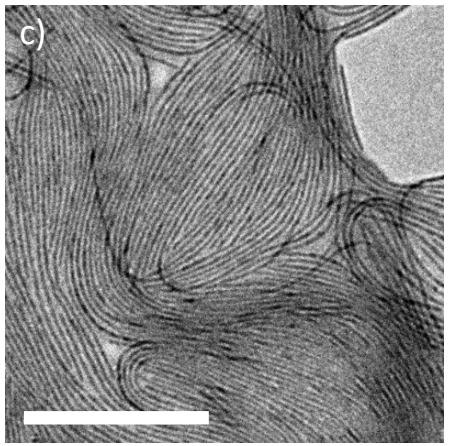

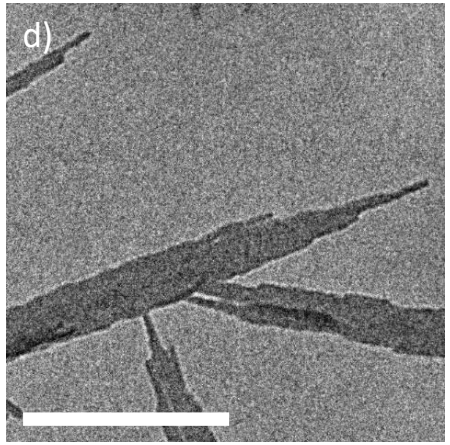

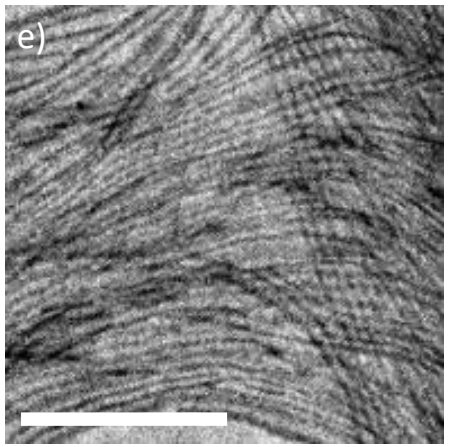

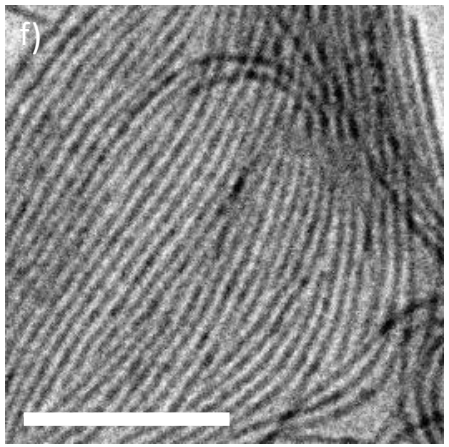

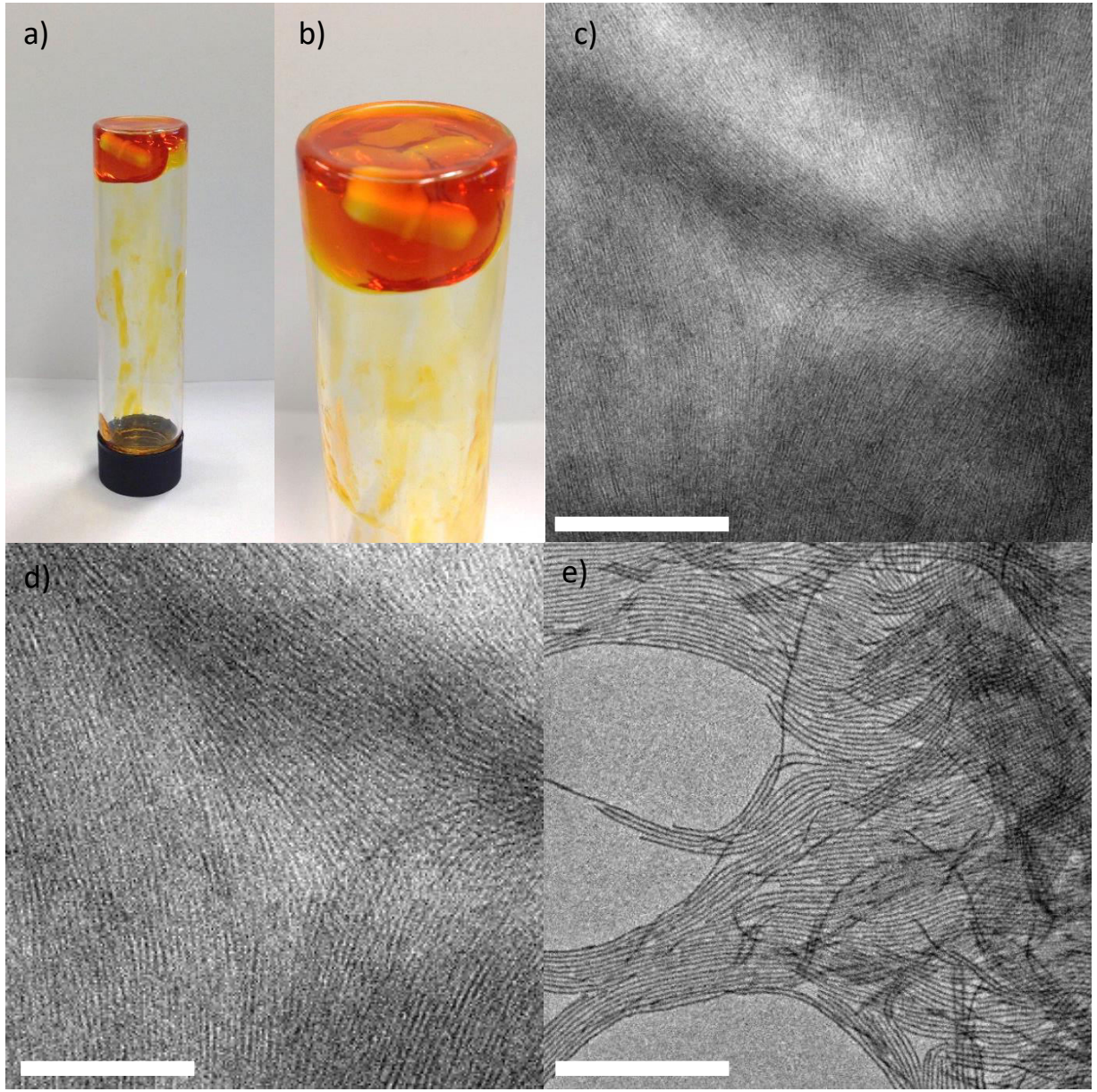
a)
b)
c)
d)
e)

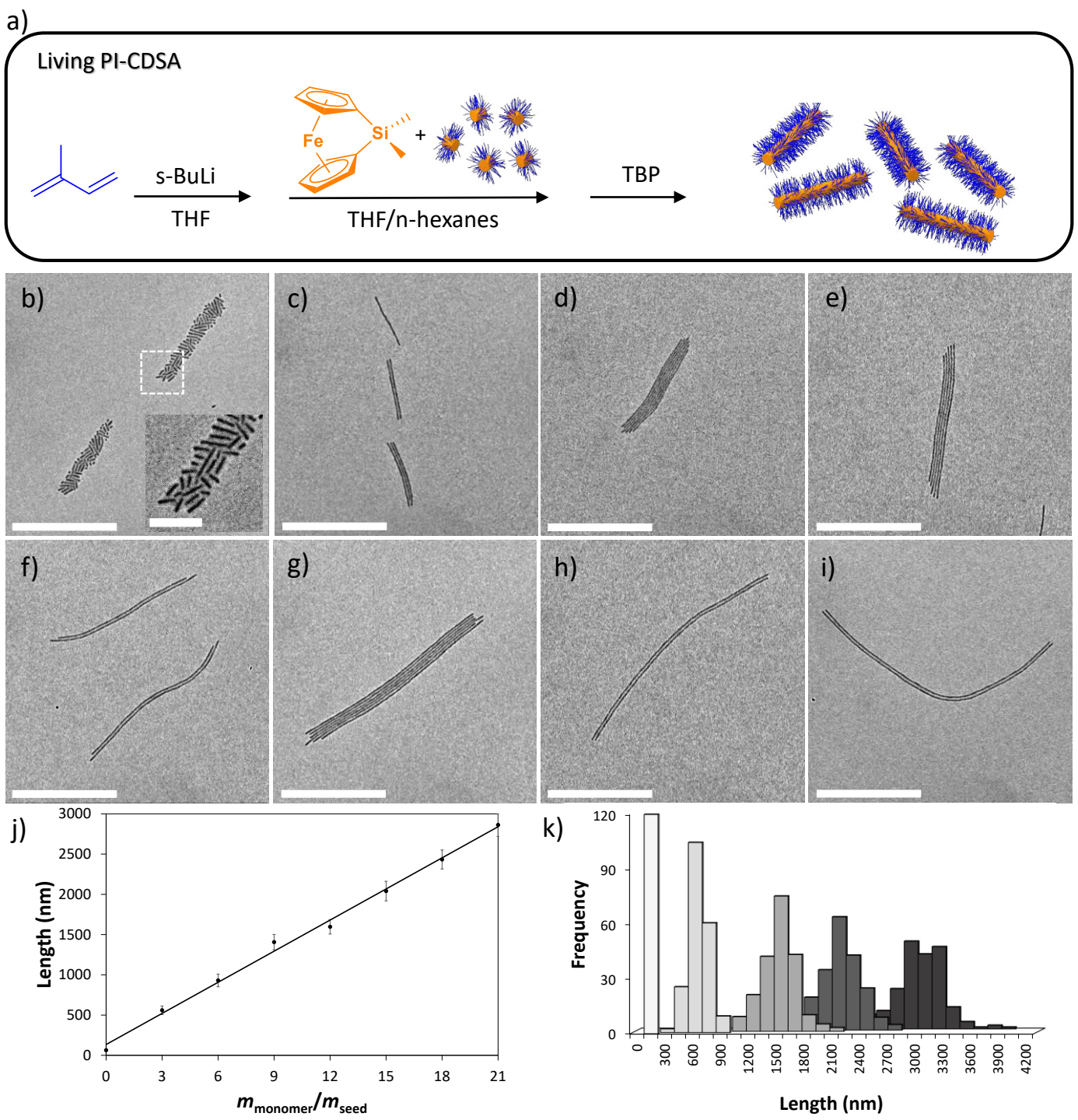
a)
Living PI-CDSA
s-BuLi
THF
Fe
Si
+
THF/n-hexanes
TBP
b)
c)
d)
e)
f)
g)
h)
i)
j)
Length (nm)
$m_{monomer}/m_{seed}$
k)
Frequency
Length (nm)

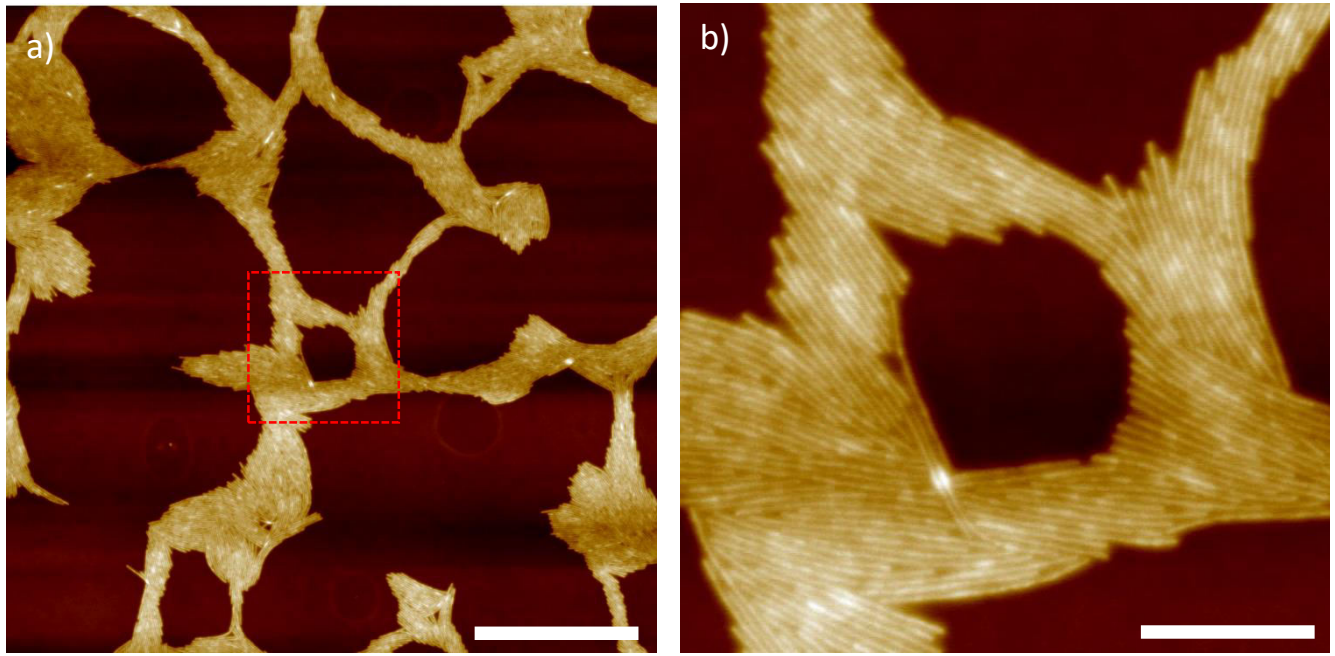
a)
b)